

Scaling Behavior in 4D Simplicial Quantum Gravity

H.S.Egawa, [†]

Department of Physics, Tokai University,
Hiratsuka, Kanagawa 259-12

T.Hotta, [‡] T.Izubuchi, [§]

Department of Physics, University of Tokyo,
Bunkyo-ku, Tokyo 113

N.Tsuda [¶]

National Laboratory for High Energy Physics (KEK)
Tsukuba, Ibaraki 305 , Japan

and

T.Yukawa ^{||}

Coordination Center for Research and Education,
The Graduate University for Advanced Studies,
Hayama-cho, Miura-gun, Kanagawa 240-01, Japan
and

National Laboratory for High Energy Physics (KEK)
Tsukuba, Ibaraki 305, Japan

Abstract

Scaling relations in four-dimensional simplicial quantum gravity are proposed using the concept of the geodesic distance. Based on the analogy of a loop length distribution in the two-dimensional case, the scaling relations of the boundary volume distribution in four dimensions are discussed in three regions: the strong-coupling phase, the critical point and the weak-coupling phase. In each phase a different scaling behavior is found.

[†]E-mail address: egawah@theory.kek.jp

[‡]E-mail address: hotta@danjuro.phys.s.u-tokyo.ac.jp

[§]E-mail address: izubuchi@danjuro.phys.s.u-tokyo.ac.jp

[¶]E-mail address: ntsuda@theory.kek.jp

^{||}E-mail address: yukawa@theory.kek.jp

1 Introduction

Two-dimensional quantum gravity has generally been regarded as a toy-model theory of four-dimensional quantum gravity. According to the Liouville theory, [1,2] two-dimensional quantum gravity can be quantized with a central charge $c < 1$. The method of dynamical triangulation [3] has generally been known as a correct discretized model corresponding to the matrix model, and has the same critical index as Liouville field theory in the continuum limit. In two dimensions many attempts, for example the so-called minbu analysis, [4,5] the loop length distributions, [6,7,8] the fractal dimensions and an analysis of the complex structures [9] reveal the many important properties of random surfaces. Especially, we take notice of the concept of the loop length distribution. Fortunately, the loop length distribution function has been calculated analytically for the case of two-dimensional pure gravity. [7,8] Our basic strategy in four dimensions is that higher-dimensional quantum gravity can be represented as a superposition of low-dimensional quantum gravity. [10] Indeed, a two-dimensional random closed surface can be reduced to a summation over the loops along a certain gauge slice regarded as the geodesic distance corresponding to time in our case. One of the aims of this article is to investigate four-dimensional Euclidean spacetime structures using the geodesic distance (precisely, the extended concept of the loop length distribution in two-dimensional simplicial quantum gravity). Based on an analogy of the loop length distribution in the two-dimensional case, the scaling relations in the four-dimensional case are discussed for three regions *i.e.* the strong-coupling phase, the critical point and the weak-coupling phase. In the three-dimensional case the scaling relations of the boundary-area distributions have already been argued using the analogy of the loop length distribution, resulting in the establishment of scaling properties. [11]

In order to discuss the scaling relations of the boundary volume, we assume that the scaling variable (x) has the form V/D^α , where V , D and α denote each boundary volume, the geodesic distance and the scaling parameter, respectively.

The rest of the article is organized as follows: section 2 briefly reviews the definition of the model. Section 3 considers the new scaling relations of the boundary volume obtained in four dimensions, and the following subsections look at these in detail for the three regions. Finally, section 4 contains a summary of the results and discussions.

2 The model

It is still not known how to give a constructive definition of four-dimensional quantum gravity. We naturally must mention the Euclidean Einstein-Hilbert action, as follows:

$$S_{EH} = \int d^4x \sqrt{g} \left(\Lambda - \frac{1}{G} R \right), \quad (1)$$

where Λ is the cosmological constant and G is Newton's constant of gravity. We use the lattice action of the four-dimensional model with the topology S^4 , corresponding to the above action, as follows:

$$\begin{aligned} S(\kappa_2, \kappa_4) &= -\kappa_2 N_2 + \kappa_4 N_4 \\ &= -\frac{2\pi}{G} N_2 + \left(\Lambda' + \frac{10}{G} \cos^{-1}\left(\frac{1}{4}\right) \right) N_4, \end{aligned} \quad (2)$$

where N_i denotes the total number of i -simplexes and $\Lambda' = c\Lambda$; c is the unit volume and $\cos^{-1}\left(\frac{1}{4}\right)$ is the angle between two tetrahedra. The coupling κ_2 is proportional to the inverse bare Newton's constant, and the coupling κ_4 corresponds to a lattice cosmological constant.

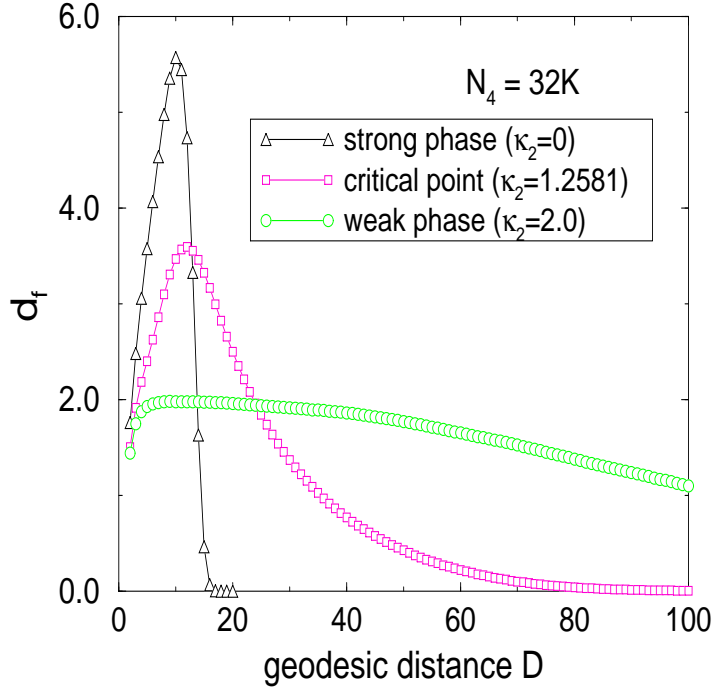


Figure 1: Fractal dimensions (d_f) versus the geodesic distance plotted for the strong phase, critical point and weak phase with $N_4 = 32K$.

For the dynamical triangulation model of four-dimensional quantum gravity we consider a partition function of the form

$$Z(\kappa_2, \kappa_4) = \sum_{T(S^4)} e^{-S(\kappa_2, \kappa_4)}. \quad (3)$$

We sum over all simplicial triangulations, $T(S^4)$, on a four-dimensional sphere. Here, we fix the topology as S^4 . In practice, we must add a small correction term, [12] ΔS , to the lattice action in order to suppress volume fluctuations. The correction term is denoted by

$$\Delta S = \delta \kappa_4 (N_4 - N_4^{(target)})^2, \quad (4)$$

where $N_4^{(target)}$ is the target value of four-simplexes, and $\delta = 0.0005$ is used.

3 Numerical simulation and results

One of the interesting observables in this model is the fractal dimension (d_f) at large scale. A common way to define the fractal dimension is based on studying the behavior of the volume within a geodesic distance D , ($V(D)$). Usually, d_f is calculated as the following quantity:

$$d_f \equiv \frac{d \ln V(D)}{d \ln D}, \quad (5)$$

which would be a constant if $V(D)$ goes like a power of D . Fig.1 denotes that the fractal dimensions are plotted versus the geodesic distances with $N_4 = 32K$. We have to inquire,

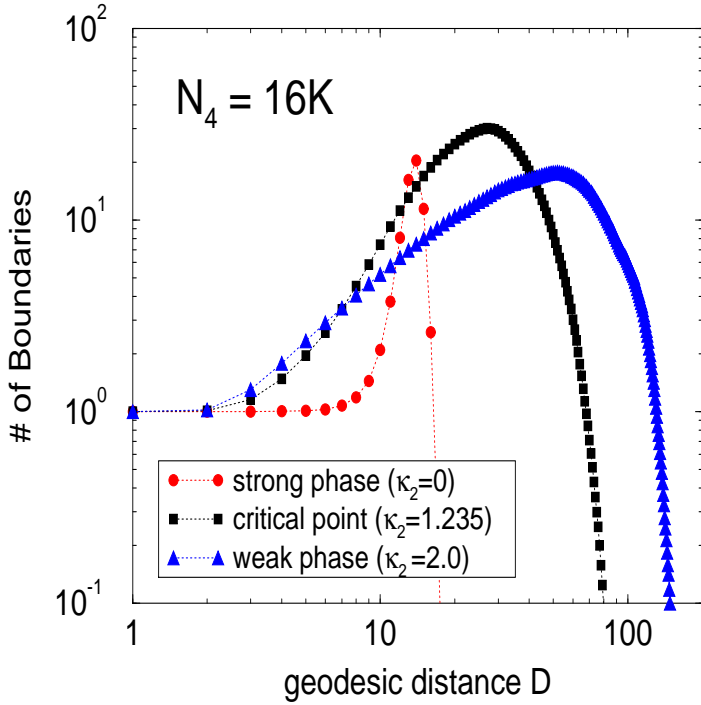


Figure 2: Number of boundaries versus the geodesic distance for the strong phase, critical point and weak phase with double-log scales.

to some extent, into the internal geometrical view points of the four-dimensional dynamically triangulated manifolds.

We define $N_b(D)$ as the number of boundaries at a geodesic distance D from a reference four-simplex in the dynamically triangulated manifolds. Fig.2 shows the distributions of $N_b(D)$ for the typical three coupling strengths with $N_4 = 16K$. In the strong-coupling limit ($\kappa_2 = 0$, this corresponds to $G \rightarrow \infty$), the only boundary that is identified as the mother universe exists within almost all of the geodesic distances; also the creation of the branches is highly suppressed, which means that the mother universe is a dominant structure. The suppression of branches shows one of the characteristic properties of a “crumpled manifold”, which is similar to the case observed in the two-dimensional manifold. On the other hand, in the weak-coupling phase (for example, we chose $\kappa_2 = 2.0$, (see Fig.2)), we see the growth of the branches (“elongated manifold”) until $D \sim 60$ for $N_4 = 16K$. From Fig.1, 2 there is no doubt that the dynamically triangulated manifold becomes crumple in the strong-coupling phase and a branched polymer in the weak-coupling phase. [13, 14]

We now devote a little more space to explaining the loop length distributions in two-dimensional dynamically triangulated surfaces. We suppose a disk which is covered within a geodesic distance of D from the arbitrary triangle. Because of the branching of the surface, a disk is not always simply-connected, and there usually appear many boundaries consisting of S^1 loops in this disk. The loop length distribution function ($\rho(L, D)$) is measured by counting the number of boundary loops with the loop length (L) within a geodesic distance (D). In ref.7) the loop length distribution function ($\rho(L, D)$) has been calculated as a function of the scaling

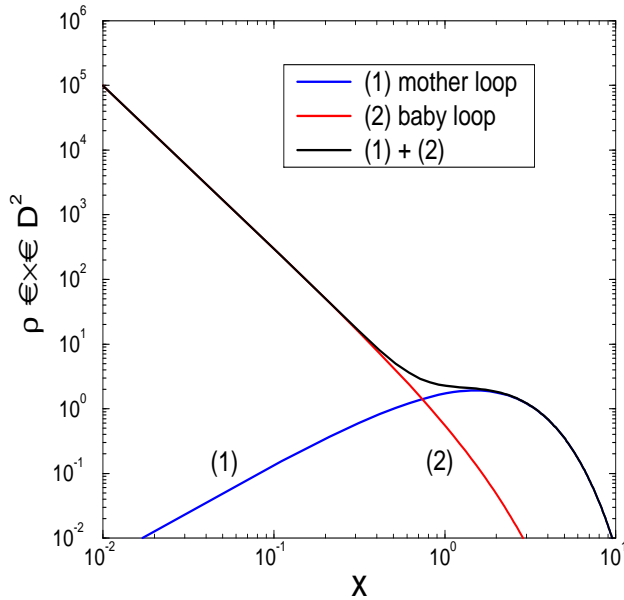


Figure 3: Loop length distribution function ($\rho(x, D)$), consisting of the mother loop and baby loops distribution function. (1)mother loop distribution function: $\frac{14}{3}x^{1/2}e^{-x}$ (thick line) and (2)baby loop distribution function: $(x^{-5/2} + \frac{1}{2}x^{-3/2})e^{-x}$ (dotted line). Both are plotted with double-log scales.

variable, $x = L/D^2$, in the continuum limit for the case of pure gravity in two dimensions,

$$\rho(x = \frac{L}{D^2}, D) = \frac{3}{7\sqrt{\pi}} \frac{1}{D^2} \left(x^{-5/2} + \frac{1}{2}x^{-3/2} + \frac{14}{3}x^{1/2} \right) e^{-x}. \quad (6)$$

This distribution function consists of two different types of distributions. The first two terms of eq.(6), $(x^{-5/2} + \frac{1}{2}x^{-3/2})e^{-x}$, represent the so-called baby loops. The baby loops originate from the quantum fluctuation of the surface.

The last term of eq.(6), $(\frac{14}{3}x^{1/2})e^{-x}$, represents the mother loop. The precise definition of the mother loop is the boundary of the largest uncovered regions for each geodesic distance. One of the notable features of the loop length distribution is that the mother loop and the baby loops distribute with the same scaling variable, $x = L/D^2$. There are also other things to note. The distribution function of the baby loops gives the divergences in the calculations of the number of boundaries at distance D , $M^0(D) = \int_0^\infty dL \rho(L, D)$, and the total length of boundaries at distance D , $M^1(D) = \int_0^\infty dL L \rho(L, D)$. These divergences indicate that $M^0(D)$ and $M^1(D)$ depend on the lattice cut-off in the model, which offers a key to understanding the universality of the distributions.

For future convenience, we show the mother and baby loop distributions in Fig.3. Similar distributions also appear in four dimensions! Numerically, these distribution functions were investigated in ref.6); excellent agreement between the numerical results and the analytical approaches has been obtained. In the sense that two distributions of the sections (or boundaries) of the surface at different distances are exactly the same as each other after a proper rescaling of the loop length, we can safely state that the dynamically triangulated surfaces become fractal.

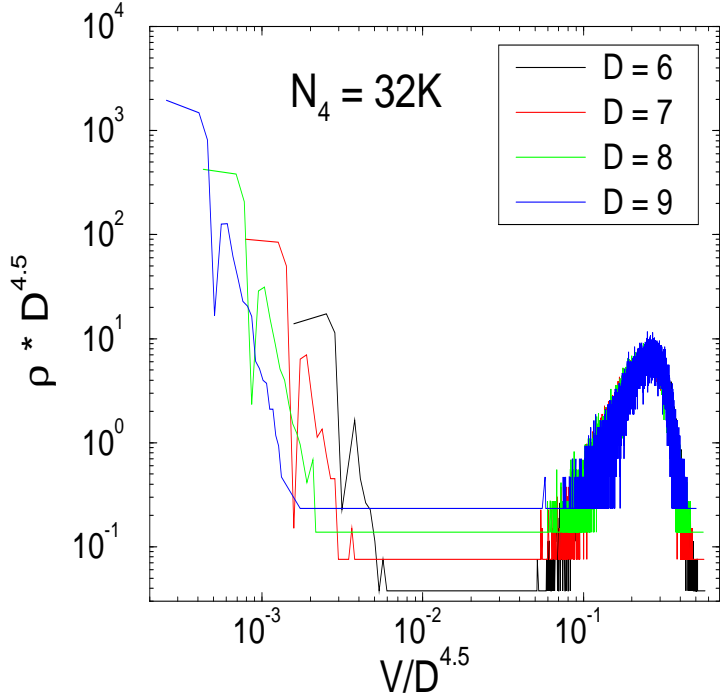


Figure 4: Boundary volume distribution in the strong-coupling limit with $N_4 = 32K$ with double-log scales.

That is to say, ρ satisfies relation (7) under rescaling, $D \rightarrow D' = \sqrt{\lambda}D$ and $L \rightarrow L' = \lambda L$,

$$\rho(x, D) \equiv \rho(L, D) = \lambda^{-1} \rho(L', D'). \quad (7)$$

We must now return to the four-dimensional case. The sections (or boundaries) of a four-dimensional dynamically triangulated manifold are closed three-manifolds. The boundary volume distribution ($\rho(x, D)$) is defined based on an analogy of the loop length distribution in two dimensions, and assuming that the scaling variable(x) has the form V/D^α , where D denotes the geodesic distance in the four-dimensional dynamically triangulated manifold.

3.1 The strong-coupling phase

Fig.4 shows the boundary volume distributions, $\rho(x) \times D^{4.5}$, with $x = V/D^{4.5}$ as the scaling variable in the strong-coupling limit, $\kappa_2 = 0$, while the fractal dimension(d_f) reaches 5.5 with $N_4 = 32K$. The boundaries of the mother universe show a good scaling property with $x = V/D^{d_f-1}$ as the scaling variable, and have a Gaussian distribution. We can recognize that in the strong-coupling phase the scaling parameter (α) of the mother universe satisfies the relation $d_f = \alpha + 1$, and that the manifold resembles a d_f -sphere (S^{d_f}), [13] where d_f denotes the fractal dimension, which increases with the volume [14](see Fig.5).

On the contrary, we have no evidence concerning the scaling properties of the volume of the baby boundaries. To be precise, it is impossible to scale the baby volumes in the same manner as the mother volume. We find a rapid increase in the distribution of the baby volumes when $x \rightarrow 0$. This rapid increase indicates the existence of the “Planck scale” in the model.

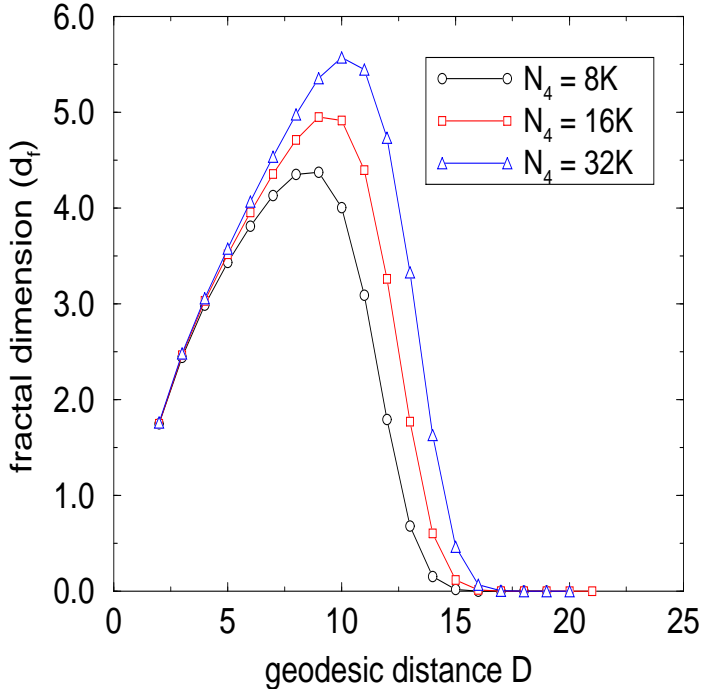


Figure 5: Fractal dimensions plotted versus the geodesic distance in the strong-coupling limit, $\kappa_2 = 0$ with $N_4 = 8K, 16K, 32K$.

3.2 The critical point

We have long believed that the phase transition in four dimensions is continuous. According to recent reports, [15] the phase transition of four-dimensional simplicial quantum gravity seems to be first order. Indeed, we have observed the double-peak structure of a histogram of N_0 in our measurements at a volume of $N_4 = 32K$ and $\kappa_2 = 1.2581$ (see Fig.6), which is a sign of a first-order transition, contrary to what is generally believed. We must draw attention to the double-peak histogram structure on the critical point. We thus measure the boundary volume distribution on both peaks, and obtain the more clear signal of the mother universe on the peak which is close to the strong-coupling phase. Fig.7 shows the boundary volume distribution on two peaks. We call the peak close to the strong-coupling phase the “down peak”, and the other peak close to the weak-coupling phase the “up peak”.

The distributions of the boundary volume obtained from the “up peak” are similar to the distributions obtained in the weak-coupling phase (see next subsection). That is to say, the structure of the mother volume disappears (see Fig.3,7). There is fairly good general agreement that the dynamically triangulated manifold behaves like a branched polymer in the weak-coupling phase. We may therefore say that the boundary volume distributions of the “up peak” are non-universal.

The data obtained in the “down peak” are shown in Fig.8 for various geodesic distances(D). We observe two different scaling properties: one is for the mother boundary, and the other is for the baby boundaries. What we have learned in two-dimensional quantum gravity is that the distribution of the mother boundary is universal, and that the baby boundaries are non-universal. We should thus notice the mother part of the distribution. Fig.9 shows the volume of

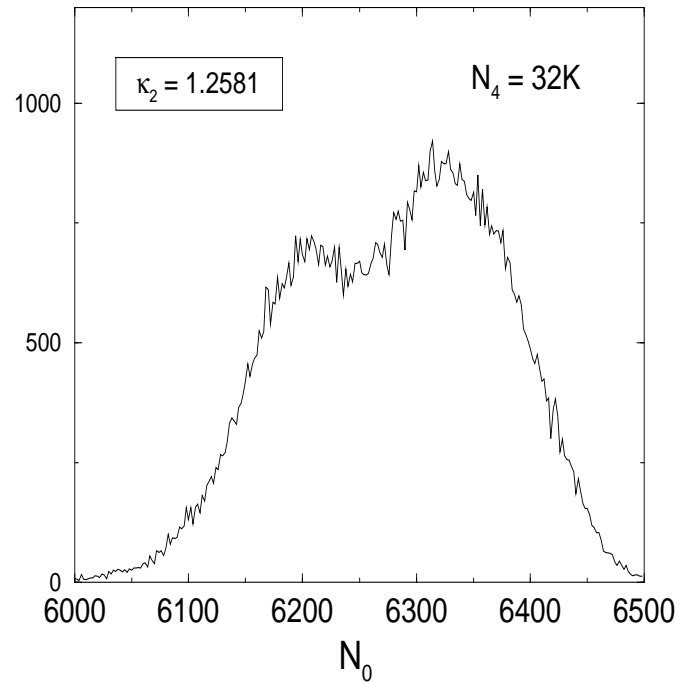


Figure 6: Histogram of V_0 at the critical point $\kappa_2 = 1.2581$ with $N_4 = 32K$.

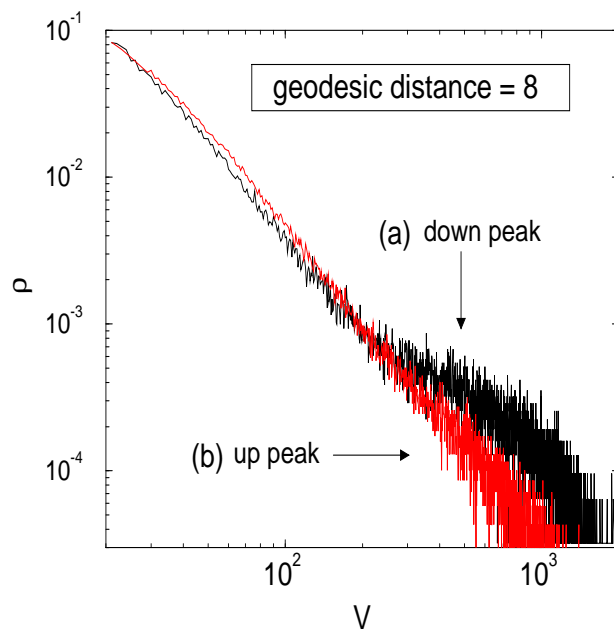


Figure 7: Boundary volume distributions of the two peaks with double-log scales. (a) denotes the boundary volume distributions of the “down peak” and (b) denotes the boundary volume distributions of the “up peak”. In the case of (b), the mother volume distribution almost disappears.

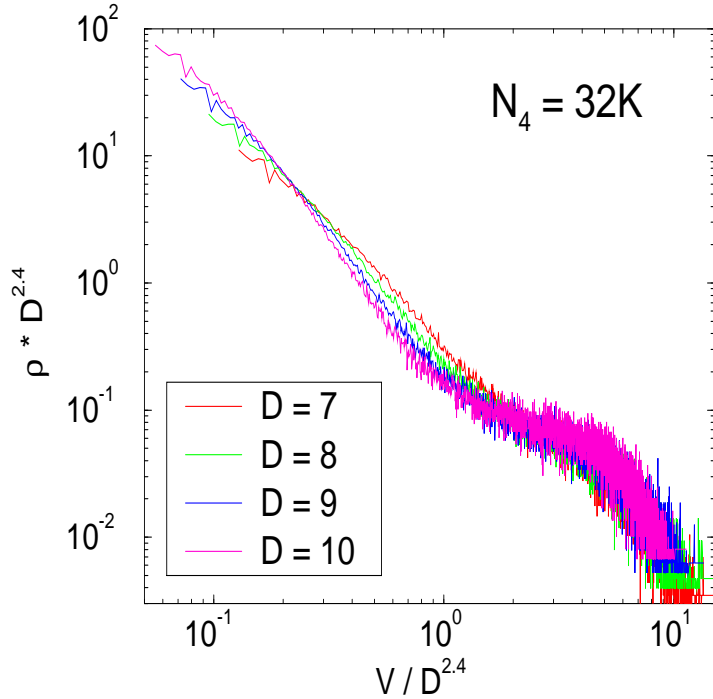


Figure 8: Boundary volume distributions with scaling variable $x = \frac{V}{D^{2.4}}$ at the critical point $\kappa_2 = 1.2581$ with double-log scales.

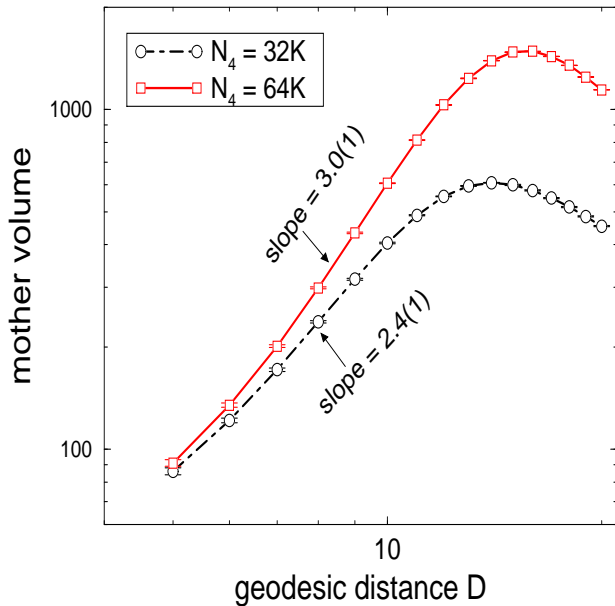


Figure 9: Volume of the mother boundary versus the geodesic distance with double-log scales at the critical point $\kappa_2 = 1.2581$ and 1.2770 with $N_4 = 32K$ and $64K$, respectively. For the case of $N_4 = 32K$ we estimate the scaling parameter $\alpha = 2.4(1)$ for the range $7 \leq D \leq 10$. For the case of $N_4 = 64K$ we also estimate the scaling parameter, $\alpha = 3.0(1)$, for the range $7 \leq D \leq 12$.

the mother boundary versus the geodesic distance at the critical points $\kappa_2 = 1.2581$ and 1.2770 with $N_4 = 32K$ and $64K$, respectively. In the case of $N_4 = 32K$, we estimate the scaling parameter $\alpha = 2.4(1)^*$ for the range $7 \leq D \leq 10$. In the case of $N_4 = 64K$ we also estimate the scaling parameter $\alpha = 3.0(1)$ for the range $7 \leq D \leq 12$. From Fig.8 we can also roughly estimate the scaling variable of the baby boundaries, $x = V/D^{4.0}$. We cannot measure the scaling parameter for the baby boundaries with the same accuracy for the mother boundary.

In order to discuss the universality of the scaling relations, we assume the distribution function in terms of a scaling parameter, $x = V/D^\alpha$, as

$$\rho(x, D) = \frac{1}{D^\alpha} x^{a_1} e^{-a_2 x}, \quad (8)$$

where a_1 and a_2 are some constants. We obtain the following expectation value of the boundary three-dimensional volume appearing at distance D :

$$\langle V^{(3)}(D) \rangle = \frac{1}{N} \int_{v_0}^{\infty} dV V \rho(x, D), \quad (9)$$

where v_0 denotes the UV cut-off of the boundary three-dimensional volume and $N = \int_{v_0}^{\infty} dV \rho(x, D)$ is a normalization factor.

If $a_1 > -1$, the right-hand side of eq.(9) converges with $v_0 \rightarrow 0$, as follows:

$$\langle V^{(3)}(D) \rangle = \frac{\Gamma(a_1 + 2)}{a_2 \Gamma(a_1 + 1)} D^\alpha, \quad (10)$$

and gives a finite fractal dimension, $d_f = \alpha + 1$. If $a_1 \leq -1$, the right-hand side of eq.(9) depends on the cut-off v_0 , and cannot give a finite value when $v_0 \rightarrow 0$. In this region, $a_1 \leq -1$, we can estimate the dominate part of this integration near to $v_0 \rightarrow 0$ for four regions, as follows:

$$\langle V^{(3)}(D) \rangle \sim \begin{cases} \left\{ a_2 \log \left(\frac{D^\alpha}{v_0} \right) \right\}^{-1} D^\alpha & \text{for } a_1 = -1 \\ v_0^{-(a_1+1)} D^{\alpha(a_1+2)} & \text{for } -2 < a_1 < -1 \\ v_0 \log \left(\frac{D^\alpha}{v_0} \right) D^{-\alpha} & \text{for } a_1 = -2 \\ v_0 D^{-\alpha} & \text{for } a_1 < -2. \end{cases} \quad (11)$$

It is clear that $\langle V^{(3)}(D) \rangle$ goes to zero when $v_0 \rightarrow 0$ whenever $a_1 \leq -1$. That is to say, the distribution with $a_1 \leq -1$ is non-universal.

We also give fractal dimensions by eq.(5),

$$d_f = \alpha + 1 \quad \text{for } -2 < a_1, \quad (12)$$

$$d_f = \alpha + 1 \quad (\text{with logarithmic correction}) \quad \text{for } a_1 = -2, \quad (13)$$

and

$$d_f = 1 - \alpha(a_1 + 1) \quad \text{for } a_1 < -2. \quad (14)$$

We can extract the function of $\rho(x, D)$ from Fig.8, and actually find $a_1 \simeq 0.5$ for the mother volume. As a result, the mother volume distribution is universal. On the other hand, we find $a_1 \simeq -2.0$ for the baby volumes. It is entirely fair to say that the distribution of the baby volumes is non-universal because it depends on the lattice cut-off (v_0). A similar non-universal distribution of the boundary volume also appears in the weak-coupling phase.

*A number inside of () is a systematic error from choices of the range of D . The determination of the range in which the mother volume expects a power law behavior of D is more or less ambiguous.

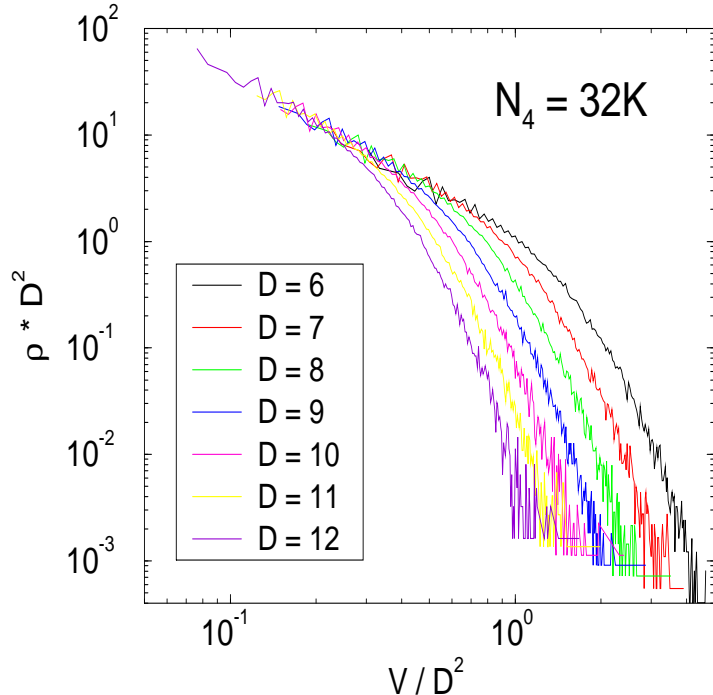


Figure 10: Boundary volume distribution in the weak-coupling phase, $\kappa_2 = 2.0$ with $N_4 = 32K$ with double-log scales.

3.3 The weak-coupling phase

In the weak-coupling phase (we chose $\kappa_2 = 2.0$), as mentioned before, the dynamically triangulated manifold resembles an elongated branched polymer; thus, we cannot observe the mother universe at all. Fig.10 shows the boundary volume distributions with $x = V/D$ as a scaling variable. Moreover, from this figure we can safely state that the $\rho(x)$ scales as

$$\rho(x) \times D \propto x^{-2.0} e^{-x}, \quad (15)$$

and that the distribution is non-universal.

For all measurements of the boundary volume distributions we prepared about 100 independent configurations on the average and 100 four-simplexes randomly in each configuration as the origin of the geodesic distance.

4 Summary and discussions

We investigated four-dimensional spacetime structures generated by dynamical triangulation using the concept of the geodesic distance. In an analogy of the loop length distribution in two-dimensional case, the scaling relations in four dimensions are discussed for the three phases *i.e.* the strong-coupling phase, the critical point and the weak-coupling phase. The boundary volume distributions ($\rho(x, D)$) give some basic scaling properties on the ensemble of Euclidean space-times described by the partition function eq.(3). In the case of two dimensions we know that the loop length distribution shows excellent agreement with an analytical prediction, [7,6] and that both of the baby loops and the mother loop show scalings with the same parameter

($x = L/D^2$). However, since the loop length distribution of the baby boundary depends on the lattice cut-off, we can recognize that it is non-universal.

The question is the boundary volume distributions in the four dimensions. In the strong-coupling limit ($\kappa_2 = 0$) we find that the mother part of the boundary volume distribution ($\rho(x, D)$) scales with $x = V/D^{d_f-1}$ as a scaling variable. In this phase there is general agreement that the four-dimensional dynamically triangulated manifold seems to be a d_f -sphere(S^{d_f}). What is important for the constructive definition of 4D simplicial quantum gravity is the fact that the boundary volume distribution of the mother universe in the strong phase gradually changes into that at the critical point. The fluctuations of the spacetime growth with $\kappa_2 \rightarrow \kappa_2^c$ and at the same time the distribution of the baby boundaries comes to scaling (see Figs.4 and 8).

At the critical point in the case of four dimensions we have obtained similar boundary volume distributions to the two-dimensional case. However, two different scaling relations are found: one is for the mother boundary ($x = V/D^{2.4}$ and $a_1 \sim 0.5$) and the other is for the baby boundaries ($x = V/D^{4.0}$ and $a_1 \sim -2$). For the reasons mentioned above, the boundary volume distribution of the mother universe seems to be universal (i.e. there is no dependence on the lattice cut-off) and that of the baby universes seems to be non-universal (i.e. there is a dependence on the lattice cut-off). We should notice that there exists a considerable size dependence of the scaling variable. In the case of $N_4 = 32K$ and $64K$ we obtain $x = V/D^{2.4(1)}$ and $V/D^{3.0(1)}$, respectively. As of now, these are all of the data in terms of the scaling variable. There is still room for further investigation.

In the weak-coupling phase we obtained elongated manifolds, in other words, the branched polymers. In this phase no mother universe exists and the boundary volume distribution of the baby universes shows a scaling relation with scaling parameters $\alpha \simeq 1.0$ and $a_1 \simeq 2.0$ (see Fig.10). However, we recognize that the distribution of the baby boundaries is non-universal.

We think that the cut-off dependence of the distribution of the baby boundaries in all the ranges of κ_2 is reflected in the existence of the Planck scale in this model. In ref.13), we see that the effective curvature increases steeply (diverges) when $D \rightarrow 0$ in all phases of κ_2 : 0.8(strong phase) $\leq \kappa_2 \leq 1.5$ (weak phase) and the authors suggest the existence of a ‘plankian regime’; $D \sim 7.5$ on grounds of the divergence. Our data of the baby boundaries are consistent with their view; also, the data of the mother and baby boundaries clear the origin of the scaling relations, which has been argued in ref.13),14). It seems reasonable to suppose that the lattice model described by eq.(3) corresponds to an effective theory which shows a rapid phase transition as well as three different types of scaling relations in each phase. [13, 15] In ref.16) we can find a discussion of another model which may have a continuous transition. For the present, it remains an unsettled question as to how to construct a consistent lattice model including “real” four-dimensional gravity in the continuum limit.

However, our numerical results are expected to be a first step to research the universal scaling relations in two-, three- and four-dimensional simplicial quantum gravity.

5 Acknowledgments

We would like to thank H.Kawai, N.Ishibashi, S.R.Das, J.Nishimura, M.Inaba and H.Hagura for fruitful discussions. We are also grateful to the members of the KEK theory group and N.Matsuhashi for advice and hospitality. Numerical calculations were performed using the HP 700 series at KEK and the Convex SPP at Tokyo Institute of Technology. Some of the authors

(T.H., T.I. and N.T.) were supported by Research Fellowships of the Japan Society for the Promotion of Science for Young Scientists.

References

- [1] V.G.Knizhnik, A.M.Polyakov and A.B.Zamolodchikov, Mod.Phys.Lett.A Vol.3 (1988) 819.
- [2] J.Distler and H.Kawai, Nucl.Phys.B 321 (1989) 509; F.David, Mod.Phys.Lett.A Vol.3 (1988) 1651.
- [3] D.Weingarten, Nucl.Phys.B 210 (1982) 229; F.David, Nucl.Phys.B 257 [FS14] (1985) 45; V.A.Kazakov, Phys.Lett.B 150 (1985) 282; J.Ambjørn, B.Durhuus and J.Fröhlich, Nucl.Phys.B 257 [FS14] (1985) 433; Nucl.Phys. B275 [FS17] (1986) 161.
- [4] S.Jain and S.D.Mathur, Phys.Lett.B 286 (1992) 819.
- [5] J.Ambjørn, S.Jain and G.Thorleifsson, Phys.Lett.B 307 (1993) 34.
- [6] N.Tsuda and T.Yukawa, Phys.Lett.B 305 (1993) 223.
- [7] H.Kawai, N.Kawamoto, T.Mogami and Y.Watabiki, Phys.Lett.B 306 (1993) 19.
- [8] N.Ishibashi and H.Kawai, Phys.Lett.B 314 (1993) 190.
- [9] H.Kawai, N.Tsuda and T.Yukawa, Phys.Lett.B 351 (1995) 162; Nucl.Phys.B (Proc.Suppl.) 47 (1996) 653; “*Complex structure of a DT surface with T^2 topology*”, [hep-lat/9609002].
- [10] G.K.Savvidy and K.G.Savvidy, Mod.Phys.Lett.A Vol.17 (1996) 1379
- [11] H.Hagura, N.Tsuda and T.Yukawa, “*Phases and fractal structures of three-dimensional simplicial gravity*”, KEK-CP 040, UTPP-45, [hep-lat/9512016].
- [12] M.E.Agishtein and A.A.Migdal, Nucl.Phys.B 385 (1992) 395.
- [13] B.V.de Bakker and J.Smit, Nucl.Phys.B 439 (1995) 239, “*Gravitational binding in 4D dynamical triangulation*”, [hep-lat/9604023].
- [14] J.Ambjørn and J.Jurkiewicz, Nucl.Phys.B 451 (1995) 643.
- [15] P.Bialas, Z.Burda, A.Krzywicki and B.Petersson, “*Focusing on the fixed point of 4d simplicial gravity*”, [hep-lat/9601024]; B.V.de Bakker, “*Further evidence that the transition of 4D dynamical triangulation is 1st order*”, [hep-lat/9603024].
- [16] W.Beirl, A.Hauke, B.Krishnan, H.Kroger, P.Homolka, H.Markum and J.Riedler, Nucl.Phys.B (Proc.Suppl.) 47 (1996) 625; R.L.Renken, “*The Renormalization Group and Dynamical Triangulations*”, [hep-lat/9610037].